Comparison of Measurement Methods to Determine the Electromagnetic Characteristics of Switched Reluctance Motors

Hélène Cailleux, Jean-Claude Mouchoux, Bernard Multon, Emmanuel Hoang, Jean-Yves Le Chenadec

Electric Drive Design and Applications (EPE Chapter Drives), Lausanne, 19-20 October 1994, pp.639-644.

COMPARISON OF MEASUREMENT METHODS TO DETERMINE THE ELECTROMAGNETIC CHARACTERISTICS OF SWITCHED RELUCTANCE MOTORS

H. Cailleux, J-C. Mouchoux, B. Multon, E. Hoang, J-Y. Le Chenadec

Laboratoire d'Electricité, Signaux et Robotique (LESiR), URA-CNRS/D1375
ENS de CACHAN, 61, avenue du Président Wilson
94235 CACHAN-Cedex, FRANCE (Tel : (33) 1 47 40 22 49 - Fax : (33) 1 47 40 21 99)

Abstract - Three different experimental methods for the electromagnetic characterization of a switched reluctance motor (SRM) are presented in this paper. Two methods rely on static measurements. The first one permits the static torque measurement when one phase of the machine is fed by a direct current. The second one determines the flux characteristic when one phase of the machine is fed at standstill by an alternative current. The third is a flux dynamic characterization method, the SRM is driven at a constant speed and fed by a direct current. Because of the emf of the motor, the feeding current is never perfectly constant especially in the case of medium and high power SRM. A numerical method is then presented which permits to compensate the effects of this current ripple. Finally, the accuracy and the feasibility of the implementation of these methods are compared.

I. INTRODUCTION

The switched reluctance motor (SRM) consists on a doubly salient brushless motor where the rotor has no windings or magnets [1]. Moreover, the currents in stator windings are unipolar. So the converter is usually composed of asymmetrical half bridges. Thus, because of this very simple structure, using SRM in numerous motion control applications becomes more and more interesting [2].

Nevertheless, because of magnetic saturation and pole shapes, the inductance of this machine depends on the stator current and on the rotor position. Then, the flux linkage of one phase and the torque are respectively functions of the current i and of the angular position θ. So, for the control and the optimization of this drive, precise magnetic characteristics are necessary [3], [4], [5]. However, authors often present comparisons of computed and measured torque and flux curves, but they rarely describe the used measurement methods. Thus in this paper, we propose different experimental methods to measure the torque or the flux arrays of the SRM. The results and the accuracy of these different methods are compared. Then the advantages and the drawbacks of each method are presented.

II. PRESENTATION OF THE STUDIED SRM

The presented measurement methods are general methods, which can be applied for the magnetic characterization of any SRM. In the paper, the SRM which has been characterized, is a Oulton PLD 112 S/2 machine (4 kW at 3000 rpm, 8/6 structure). The rotor of this four phases SRM has 6 teeth. The position sensor resolution is 900×4 points per revolution (600 pt per electrical period).

Assuming no magnetic coupling between phases (this hypothesis will be examined in chapter III 2), the electrical and mechanical dynamics are given by the following equations:

$$u_k = Ri_k + \frac{d\psi_k(\theta, i_k)}{dt} \qquad k = 1, 2, \ldots, q \tag{1}$$

$$T(\theta, i_1, i_2, \ldots, i_q) - T_l = J\frac{d\Omega}{dt}$$

$$\text{with} \quad T(\theta, i_1, i_2, \ldots, i_q) = \sum_{k=1}^{q} T_k(\theta, i_k) \tag{2}$$

where u_k is the stator voltage, i_k the current of the k phase, R the stator resistance, q the number of phases, θ and Ω the mechanical position and speed, ψ the flux in the machine, T the total torque produced by the machine, T_k the torque produced by the phase k, T_l the load torque and J the inertia of the drive. The necessity to characterize precisely the flux function ψ(θ,i) and the torque function T(θ,i) appears in (1) and (2). Without a good knowledge of the magnetic characteristic of the machine, its electrical and mechanical behaviours cannot be determined.

According to electrical machine theory, the motor torque can be deduced from the flux measurements (and vice versa) as follows:

$$W'em_k(\theta, i_k) = \int_0^{i_k} \psi_k(\theta, i)\,di \tag{3}$$

$$T_k(\theta, i_k) = \frac{\partial W'em_k(\theta, i_k)}{\partial\theta} \tag{4}$$

where W'em is the magnetic coenergy.

If the rotor and the stator have symmetric structures and if the magnetic losses are negligible, then the flux is an even function of the position and the torque is an odd function of the position. These properties allow the experimental study on half an electrical period. Furthermore, in the paper, the validity of the no magnetic coupling (between phases) hypothesis and the negligible magnetic losses hypothesis will be discussed.

Electric Drive Design and Applications (EPE Chapter Drives), Lausanne, 19-20 October 1994, pp.639-644.

III. DIRECT STATIC MEASUREMENT OF TORQUE

The rotor of the studied machine is jammed on a chosen position. One of the four phases of the motor is fed by a direct current. The torque produced by this fed phase is transmitted by a lever arm to a force sensor. The horizontality of the lever arm has to be controlled (α very small) in order that the force F is an accurate measure of the torque T (fig. 1). The force sensor is constituted by strain gauges whose range is 10 daN. As shown on fig. 1, the torque is obtained by: $T=F.d.\cos\alpha \approx F.d$.

The static torque measurement are realised for rotor positions chosen between 0 and 180 electrical degrees. The unaligned position corresponds to 0° and the conjunction position to 180°. The value of the feeding direct current varies between 0 and 15 A. The obtained torque characteristics are presented on fig. 2 (0, 1.5 A, 3 A,…, 15 A).

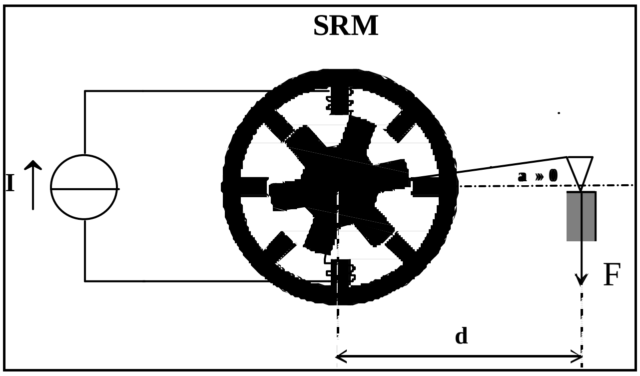

Fig. 1: Static torque measurement bench

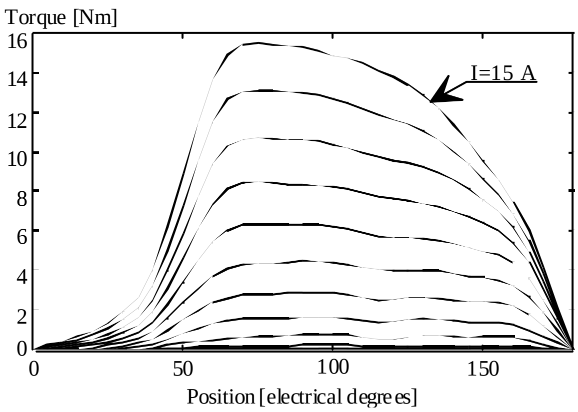

Fig. 2: Static single phase electromagnetic torque characteristics

1) Deduction of the flux characteristics: The flux characteristics can be deduced from the torque and the unaligned flux characteristic $\psi(0,i)$. By numeric integration, the magnetic coenergy can be calculated as follows:

$$W'em(\theta_o, i_o) = \int_0^{\theta_o} T(\theta, i_o) d\theta + Lo \frac{i_o^2}{2} \tag{5}$$

The Lo inductance is determined by measuring the flux in the machine with a static method (cf. § IV) for the unaligned position. Lo corresponds to the slope of the $\psi(0,i)$ characteristic. In the singular case where the magnetic circuit saturates even in the unaligned position, the equation (5) will become:

$$W'em(\theta_o, i_o) = \int_0^{\theta_o} T(\theta, i_o) d\theta + W'em(0, i_o) \tag{6}$$

The corresponding flux is deduced by numeric derivation:

$$\psi(\theta_o, i_o) = \frac{\partial W'em(\theta_o, i_o)}{\partial i} \tag{7}$$

The obtained flux linkage characteristics are presented on fig. 3 (0, 1 A, 2 A,…, 15 A).

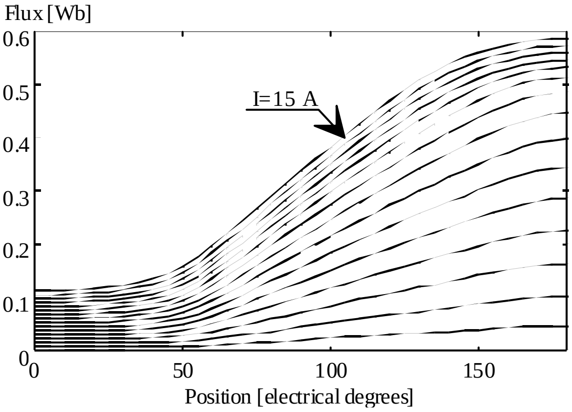

Fig. 3: Deduced flux linkage from the static torque

2) Study of the magnetic coupling: The coupling effects are studied by feeding two consecutive phases at the same time. The total torque produced by the motor, is measured for different positions with the previous method and is represented on fig. 4. In this example, one phase has been fed at +15 A for each measure point. In the second phase, the current values have been adjusted between 0 and 15 A.

The total torque wave forms obtained when the first phase is supplied at +15 A (case 1) and at -15 A (case 2) are compared with the sum of the single phase torque wave forms of each phase, fed with the same currents (case 3) (fig. 5). Without magnetic coupling, the cases 1, 2 and 3 will be equivalent. According to the results of the fig. 5, the magnetic coupling are not very important for the studied machine. The maximal difference between the torque of the cases 1 and 3 is 12% whereas the maximal difference between the torque of the cases 2 and 3 is 7%. In the case 1, the flux produced by the +15 A fed coil circulates in a long part of the yoke with the same sense as the flux produced by the other phase. Consequently, a long part of the yoke is more saturated in the case 1, then the total torque wave form is lower. In the case 2, the flux produced by the two phase circulate in the long part of the yoke with opposite senses. The saturation provides a lower effect and the total torque wave form is nearly equal to the sum of the corresponding single phase torque wave forms.

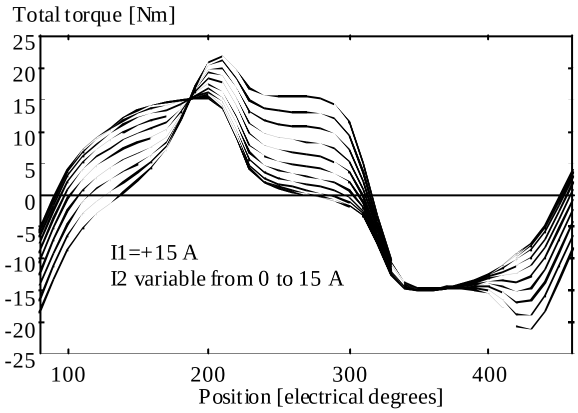

Fig. 4: Total torque wave forms for two fed phases

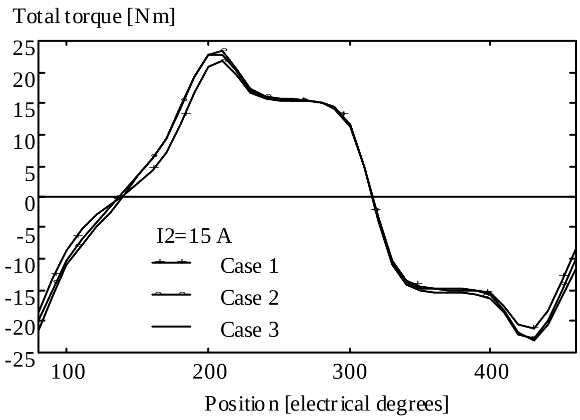

Fig. 5: Total torque for different feeding cases

IV. DIRECT STATIC MEASUREMENT OF FLUX LINKAGE ARRAY

We propose three experimental methods to measure the flux array. The first one consists in winding a sense coil around the stator teeth of the fed phase and in measuring the induced voltage. The flux is deduced from the measured induced voltages by a numeric integration. Numbers of turns of the phase and sense windings have to be known. If the stator poles are not accessible, the induced voltage can be deduced from the feeding voltage by compensating the resistive effect. For bifilar winding motor, the last method consists by feeding one winding and by measuring the induced voltage provided by the second one. The first presented flux measurement method has been used for the characterization of our motor. The rotor of the studied machine is jammed on a chosen position θ. One of the four phases of the motor is fed by a tension amplifier with an alternative current. To limit core losses effects, the phase is supplied with a low frequency generator (1 Hz). But a 50 Hz mains supply is also possible, and it is desirable in the case of high power SRM. The current amplitude varies between -15 A and +15A. The induced voltage is integrating by a digital acquisition system (fig. 6). The hysteresis loop for the conjunction position is represented on fig. 7. If the frequency of the feeding current is low enough, then the hysteresis loop is narrow and the eddy current effects can be neglected. The final flux is obtained by averaging the hysteresis loop.

The flux characteristics deduced from these static measures are presented on fig. 8. The torque characteristics can be calculated from these flux static measurements by applying the equations (3) and (4).

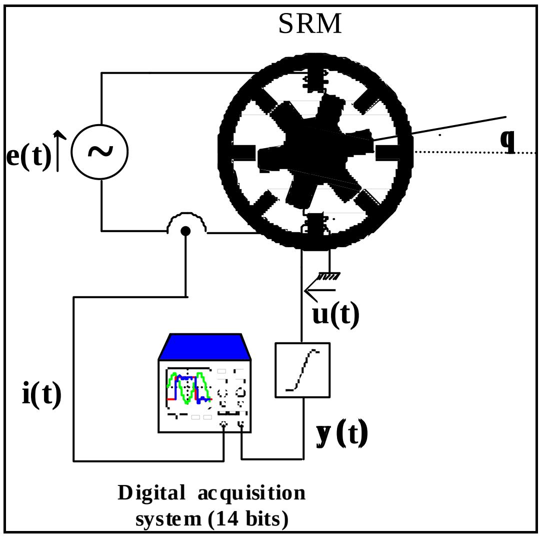

Fig. 6: Static flux measure bench

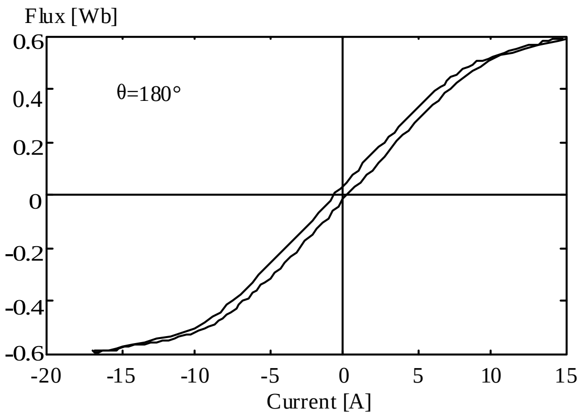

Fig. 7: Hysteresis loop for the conjunction position

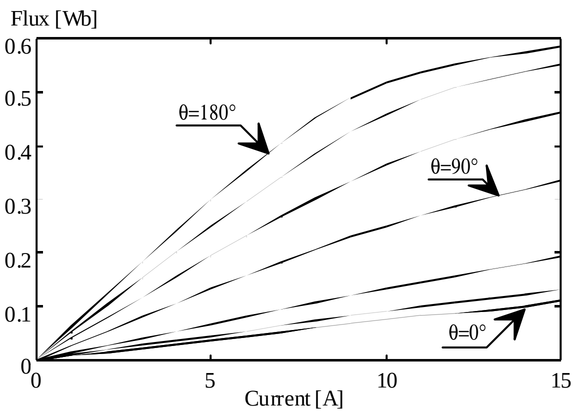

Fig. 8: Static flux characteristics

Electric Drive Design and Applications (EPE Chapter Drives), Lausanne, 19-20 October 1994, pp.639-644.

V. DYNAMIC MEASUREMENT OF INDUCED VOLTAGE

The same remark as the previous chapter one, about the different methods for the induced voltage measurement, can be said. The studied SRM is driven at a constant speed (500 rpm). The choice of the speed results from the compromise between a low speed ripple and a low effect of the magnetic losses. One of the four phases of the SRM is fed by a direct current (fig. 9). The induced voltage is then measured. On the fig. 10 are represented the feeding current and the corresponding induced voltage for a mean current of 15 A. The flux array is calculated as follows:

As $u(t) = \frac{n_s}{n} * \frac{d\psi(t)}{dt}$ then:

$$\psi(\theta_o, i_o) = \frac{n}{n_s} \cdot \int_0^{\theta_o} u(\theta) \cdot d\theta + \psi(0, i_o) \qquad (8)$$

where n and n_s are respectively the number of turns of the phase and sense coils.

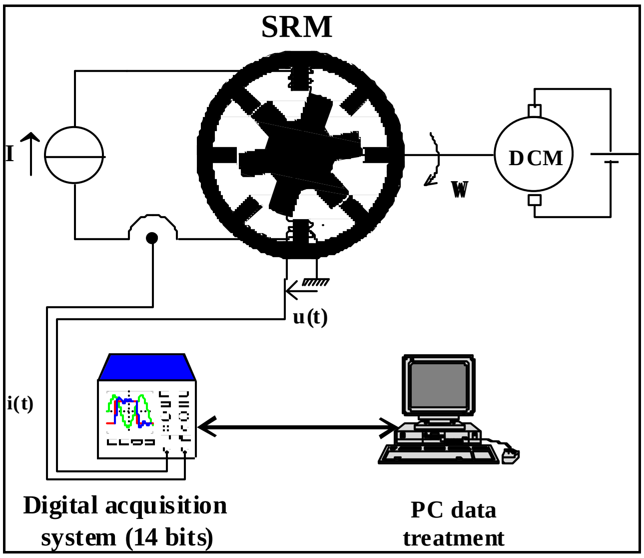

Fig. 9: Dynamic induced voltage measure bench

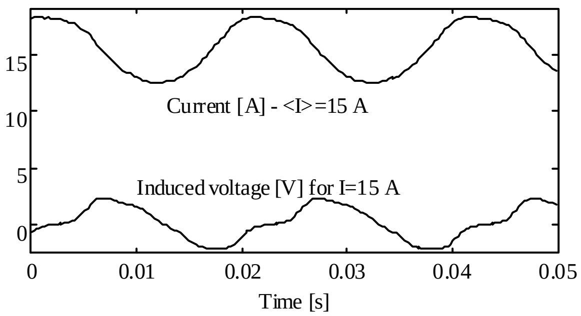

Fig. 10: Current and induced voltage shapes

The results are satisfactory if the ripple of the current is negligible. But inevitable ripple disturbs the current because of the emf of the machine (see fig 10). A numeric method has been developed to compensate this current ripple effect.

1) The numeric compensation method: For each set of measurements at a given current value i_m, the current is disturbed. The first part of the compensation is to calculate the corrected induced voltage, $u_m$cor, for a constant current $<i_m>$ by using a linear interpolation where $<i_m>$ is the average value of all the currents i_m (see fig. 11):

$$u_m cor = u_m + \frac{(u_m - u_{m-1})}{(i_m - i_{m-1})} * (< i_m > - i_m) \qquad (9)$$

With these corrected induced voltages $u_m$cor, a first calculus of the flux is realised ($\psi^o(\theta,i)$) as in (8).

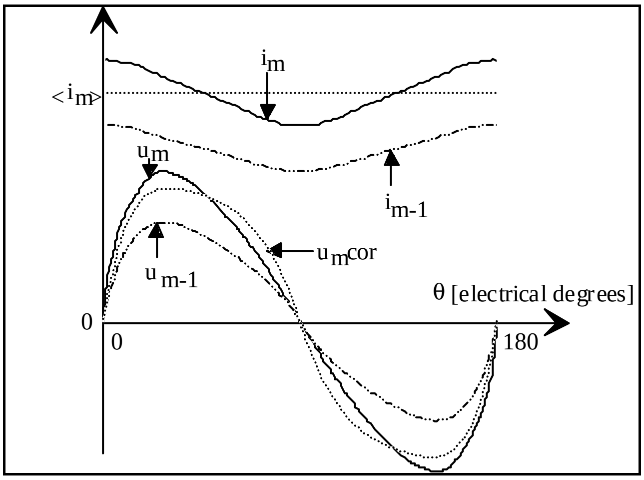

Fig. 11: Corrected induced voltage calculation

The induced voltage of the sense coil can be written as follows:

$$u_m cor = \frac{n_s}{n} * \frac{d\psi}{dt} = \frac{n_s}{n} * \left(\frac{\partial\psi}{\partial i} * \frac{di}{dt} + \frac{\partial\psi}{\partial\theta} * \frac{d\theta}{dt}\right) \qquad (10)$$

Because of the current ripple, the first term of the equation is not equal to zero ($di/dt \neq 0$). The compensation of the ripple current can be written as follows:

$$\frac{\partial\psi}{\partial\theta} * \frac{d\theta}{dt} = \left(u_m cor * \frac{n}{n_s}\right) - \left(\frac{\partial\psi}{\partial i} * \frac{di}{dt}\right) \qquad (11)$$

Then, the calculus of the corrected flux is:

$$\psi(\theta, i) = \int_0^{\theta} \left(u_m cor \frac{n}{n_s} - \frac{\partial\psi}{\partial i} \cdot \frac{di}{dt}\right) \cdot d\theta + \psi(0, i) \qquad (12)$$

Furthermore, the flux $\psi(\theta_p, i_m)$ can be deduced from the flux $\psi(\theta_{p-1}, i_m)$ as follows (see fig. 12):

$$\psi(\theta_p, i_m) = \psi(\theta_{p-1}, i_m) + \int_{\theta_{p-1}}^{\theta_p} \left(u_m cor \frac{n}{n_s} - \frac{\partial\psi}{\partial i} \cdot \frac{di}{dt}\right) \cdot d\theta \qquad (13)$$

with $\Delta\theta = \theta_p - \theta_{p-1}$

By a numeric integration, the equation becomes:

$$\psi(\theta_p, i_m) = \psi(\theta_{p-1}, i_m) + \left(u_m cor \frac{n}{n_s} \Delta\theta - \frac{\Delta\psi}{\Delta i}(i_m(\theta_p) - i_m(\theta_{p-1}))\right) \qquad (14)$$

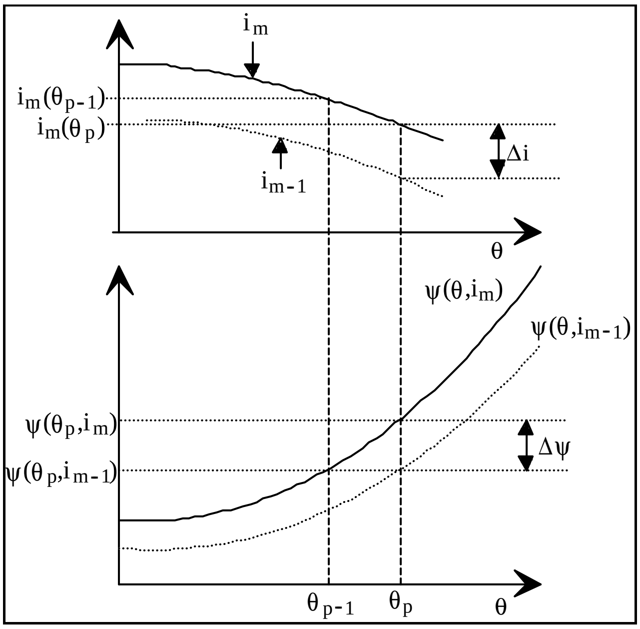

Fig. 12: Corrected flux calculation

To take account the influence of current ripple, we have to realize an iterative computation procedure. The di/dt is equal to zero at the unaligned position (θ=0°), then $\psi^0(0,i)$ needs no compensation (see fig. 11). The next value of the corrected flux $\psi^1(\theta,i)$ are deduced from $\psi^0(0,i)$ in applying (14). Only a few iterations are necessary because the result converges quickly.

2) Results: On fig. 13, the flux calculated by integrating the induced voltage as in (8) is compared with the flux obtained with the previous numeric method which compensates the current ripple. The final amplitude of the corrected flux is superior to the other one. On fig. 14, the amplitude of the torque deduced from the corrected flux is better. To improve this numeric method for the flux calculation, the asymmetry of the induced voltage due to the magnetic losses has to be studied.

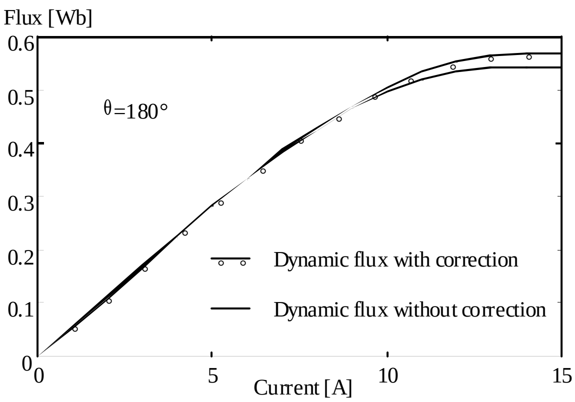

Fig. 13: Comparison of the dynamic flux

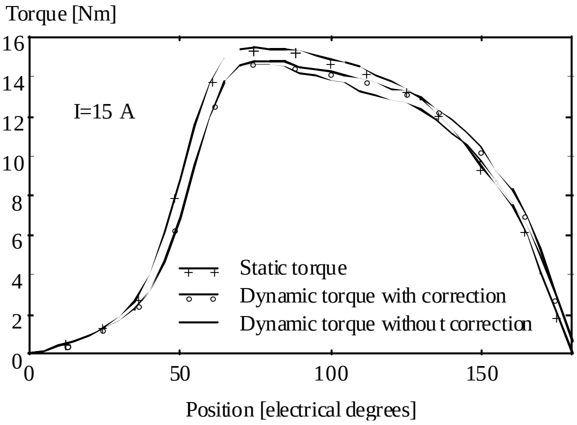

Fig. 14: Comparison of the torque wave forms deduced from the dynamic flux

VI. COMPARISON OF THE MEASUREMENT METHODS

1) Accuracy of the results: On fig. 15-18, the results of the three experimental electromagnetic characterization methods are compared.

These three methods give similar results for the flux characteristic determination. The flux characteristic obtained with the compensated dynamic method is always lower than the flux characteristics obtained with the two static methods. The magnetic losses produced when the machine is driven and perhaps the speed ripple, can explain these lower performances (fig. 15-16).

The static torque characteristic and the torque characteristic deduced from the dynamic flux measurement are similar (fig.17). Nevertheless the dynamic torque amplitude is lower than the static torque one (magnetic losses). The results of the torque deduced from the flux static measurement seem less satisfactory. Indeed, the flux static measures has been realised for a few values of position. Then, the numeric derivation of the magnetic coenergy with regard to the position is not precise enough. Otherwise, the static torque/current characteristic and the torque/current characteristic deduced from the static flux measurement are very similar (fig. 18).

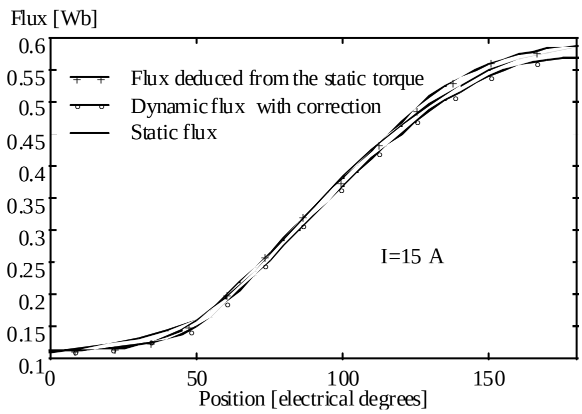

Fig. 15: Comparison of the flux/position characteristics

Electric Drive Design and Applications (EPE Chapter Drives), Lausanne, 19-20 October 1994, pp.639-644.

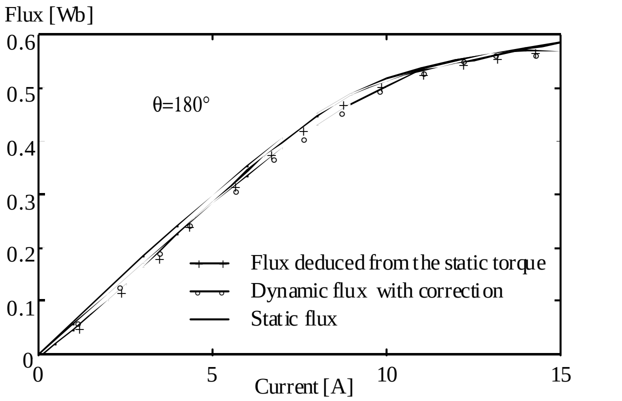

Fig. 16: Comparison of the flux/current characteristics

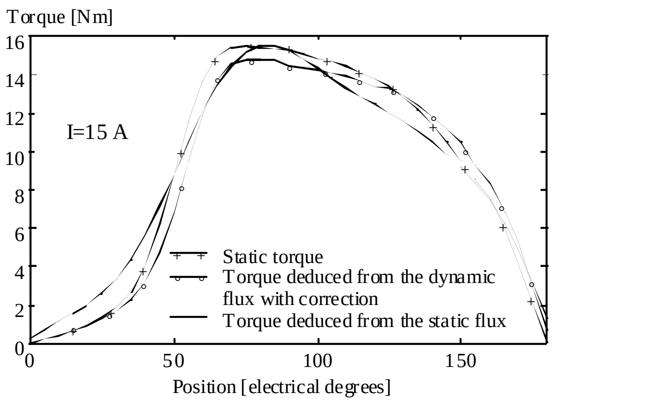

Fig. 17: Comparison of the torque/position characteristics

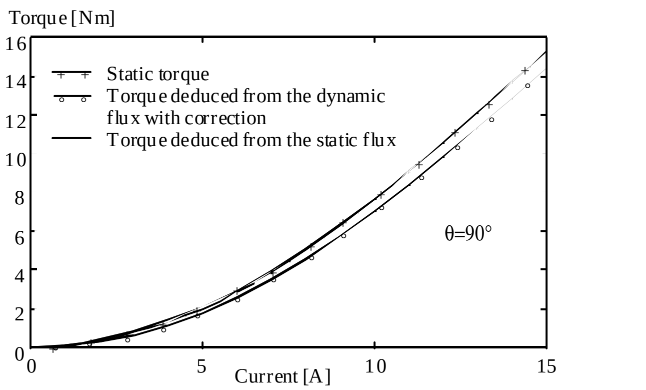

Fig. 18: Comparison of the torque/current characteristics

2) Easiness of the implementation: The direct static measurement of torque is a very precise method but it needs a special measurement equipment (force sensor, mechanical system to jam the machine in the chosen position). The measurement is long because for a precise torque array, the measures have to be repeated for a lot of positions. The deduction of the flux array is satisfactory (cf. table 1).

The direct static measurement of flux method is precise but long (adjustment of the mechanical system to jam the machine in a position for each set of measures). The deduction of the torque array is acceptable (cf. table 1).

The dynamic measurement of induced voltage is the fastest method to characterize the flux array of a SRM. The results are satisfactory if the current ripple is taken into account. The deduction of the torque array is acceptable (cf. table 1).

	Flux characterization	Torque characterization
Direct static measurement of torque	satisfactory	very precise long force sensor
Direct static measurement of flux array	precise long acquisition system	acceptable
Dynamic measurement of induced voltage	satisfactory fast acquisition system	acceptable

Table 1: Recapitulation of measurement method qualities

VII. CONCLUSION

The dynamic measurement of induced voltage seems to be the characterization method for which the compromise between the accuracy and the easiness of implementation is the best. With a digital data acquisition system, the flux/position/current characteristics can be determined very quickly. Furthermore, with the current ripple compensation method, the feeding current doesn't need to be perfectly smooth. For the flux characterization of high power machine, this method permits to avoid the use of important choke. But it will probably be necessary to take account the magnetic losses and the speed ripple to obtain very good results.

Otherwise the torque static measurement remains the more precise method for the electromagnetic characterization of SRM. For instance, this method is strongly advised to determine the model which will be used afterwards for the control of the machine.

VIII. REFERENCES

[1] LAWRENSON P. J., STEPHENSON J. M., BLENKINSOP P. T., CORDA J., FULTON N. N., *Variable-speed switched reluctance motors*, IEE Proc., Vol. 127, Pt. B, No. 4, July 1980, pp. 253-265.

[2] MILLER T. J. E., *Brushless permanent-magnet and reluctance motor drives*, Oxford Science Publications, 1989.

[3] FERRERO A., RACITI A., URZI C., *An indirect test method for the characterization of variable reluctance motors*, IEEE Trans. on Ins.. and Measurement, Vol. 42, No. 6, December 1993, pp. 1020-1025.

[4] CORDA J., MASIC S., STEPHENSON J.M., *Computation and experimental determination of running torque waveforms in switched-reluctance motors*, IEE Proc.-B, Vol. 140, No. 6, November 1993.

[5] FERRERO A., RACITI A., *A digital method for the determination of the magnetic characteristic of variable reluctance motors*, IEEE Trans. on Instrumentation and Measurement, Vol. 39, No.4, August 1990, pp. 604-608.